SECURITY CLASSIFICATION OF THIS PAGE

(2)

AD-A242 574

REPORT DOCUMENTATION PAGE

	1b. RESTRICTIVE MARKINGS
2b. DECLASSIFICATION / DOWNGRADING SCHEDULE	3. DISTRIBUTION / AVAILABILITY OF REPORT Approved for public release; distribution unlimited
4. PERFORMING ORGANIZATION REPORT NUMBER(S) Report # 1	5. MONITORING ORGANIZATION REPORT NUMBER(S)
6a. NAME OF PERFORMING ORGANIZATION Washington University	6b. OFFICE SYMBOL (If applicable)
6c. ADDRESS (City, State, and ZIP Code) One Brookings Drive St. Louis, MO 63130-4899	7a. NAME OF MONITORING ORGANIZATION Office of Naval Research
	7b. ADDRESS (City, State, and ZIP Code) 800 N. Quincy Street Arlington, VA 22217-5000
8a. NAME OF FUNDING / SPONSORING ORGANIZATION ONR	8b. OFFICE SYMBOL (If applicable)
8c. ADDRESS (City, State, and ZIP Code) 800 N. Quincy Street Arlington, VA 22217-5000	9. PROCUREMENT INSTRUMENT IDENTIFICATION NUMBER N00014-90-J-4118; R&T Code (413MØØ1)
	10. SOURCE OF FUNDING NUMBERS PROGRAM ELEMENT NO. / PROJECT NO. / TASK NO. / WORK UNIT ACCESSION NO

11. TITLE (Include Security Classification)
Selective Observation of the Interface of Heterogeneous Polycarbonate/Polystyrene Blends by Dynamic Nuclear Polarization C-13 NMR

12. PERSONAL AUTHOR(S)
Mobae Afeworki, Robert A. McKay, and Jacob Schaefer

13a. TYPE OF REPORT	13b. TIME COVERED	14. DATE OF REPORT (Year, Month, Day)	15. PAGE COUNT
Technical	FROM _____ TO _____	11/14/91	42

16. SUPPLEMENTARY NOTATION

17. COSATI CODES			18. SUBJECT TERMS (Continue on reverse if necessary and identify by block number)
FIELD	GROUP	SUB-GROUP	Heterogeneous Blends; polycarbonate; polystyrene; dynamic nuclear polarization; magic-angle spinning ^{13}C NMR; interface.

19. ABSTRACT (Continue on reverse if necessary and identify by block number)

Heterogeneous blends of [3,3′-$^{13}C_2$]polycarbonate and [ul-ring-$^{12}C_6$]polystyrene were formed by serial film casting. The polystyrene phase of each blend was homogeneously doped with 2% by weight of a bisdiphenylenephenylallyl free-radical complex with benzene. Proton polarization enhanced by dynamic nuclear polarization was generated in the polycarbonate phase by dipolar coupling to electrons in the polystyrene phase under 39-GHz microwave irradiation at the difference of the electron and proton Larmor frequencies. Proton magnetization was then transferred to carbons under matched, spin-lock conditions for detection with chemical-shift selectivity by magic-angle spinning ^{13}C NMR. The ^{13}C signal from polycarbonate arises exclusively from chains which are at the polycarbonate/polystyrene interface. Signals from bulk polycarbonate were suppressed by differencing techniques. Attempts at direct polarization transfers from electrons in the polystyrene phase to carbons in the polycarbonate phase failed.

20. DISTRIBUTION / AVAILABILITY OF ABSTRACT	21. ABSTRACT SECURITY CLASSIFICATION	
☒ UNCLASSIFIED/UNLIMITED ☐ SAME AS RPT. ☐ DTIC USERS		
22a NAME OF RESPONSIBLE INDIVIDUAL Dr. Jacob Schaefer	22b. TELEPHONE (Include Area Code) 314-935-6844	22c. OFFICE SYMBOL

DD FORM 1473, 84 MAR 83 APR edition may be used until exhausted. All other editions are obsolete.

SECURITY CLASSIFICATION OF THIS PAGE

I. Selective Observation of the Interface of Heterogeneous Polycarbonate/Polystyrene Blends by Dynamic Nuclear Polarization C-13 NMR

Mobae Afeworki†, Robert A. McKay, and Jacob Schaefer

Department of Chemistry
Washington University
St Louis, MO 63130

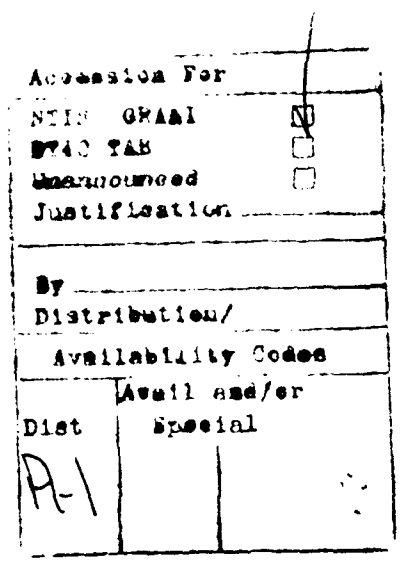

†Present address: Exxon Research and Engineering Company, Annandale, NJ 08801

ABSTRACT

Heterogeneous blends of [3,3'-$^{13}C_2$]polycarbonate and [ul-ring-$^{12}C_6$]polystyrene were formed by serial film casting. The polystyrene phase of each blend was homogeneously doped with 2% by weight of a bisdiphenylenephenylallyl free-radical complex with benzene. Proton polarization enhanced by dynamic nuclear polarization was generated in the polycarbonate phase by dipolar coupling to electrons in the polystyrene phase under 39-GHz microwave irradiation at the difference of the electron and proton Larmor frequencies. Proton magnetization was then transferred to carbons under matched, spin-lock conditions for detection with chemical-shift selectivity by magic-angle spinning ^{13}C NMR. The ^{13}C signal from polycarbonate arises exclusively from chains which are at the polycarbonate/polystyrene interface. Signals from bulk polycarbonate were suppressed by differencing techniques. Attempts at direct polarization transfers from electrons in the polystyrene phase to carbons in the polycarbonate phase failed.

INTRODUCTION

Blends of Immiscible Polymers: Many new commercial engineering materials are blends of incompatible polymers. These blends often have a mix of the performance characteristics of each of the components. Applications of heterogeneous polymer blends range from strong, lightweight automobile parts to dental glues [1]. The mechanical properties of the blends depend upon the mixing of the components. Existing theories of blending of immiscible polymers are not detailed, but envision the formation of homopolymer microdomains with dimensions between 10 and 100 Å [2]. We believe that progress in gaining an understanding of the mechanical properties of such heterogeneous blends depends upon experimental characterization of the interfacial regions.

Here we make the distinction between the "interface" and "interphase" of polymer blends. The interface between two immiscible polymers is defined as a sharp boundary with no intermixing of chains. Despite this separation, chain packing and dynamics in the regions on either side of this interfacial boundary may differ from those of the bulk homopolymers. The interphase is "a region of interdiffusion" [3] of two immiscible polymers that arises from kinetic trapping and intermingling of chains during coprecipitation or heating above T_g's. The blend-sample preparation technique used in this work involves interfacial regions only.

Analyzing the Interfacial Region: Characterization of the interfaces and interphases of immiscible polymer blends in the past has involved techniques such as thermal analysis [4], transmission electron microscopy [5], small angle x-ray [6] or neutron [7] scattering, and non-radiative

transfer of fluorescent labels [8]. Thermal analysis can be useful for some pairs of immiscible polymers but does not provide microscopic insight into the structure of the interface. Imaging of the blend domains is made impractical by domain sizes less than 50 Å. Data reduction for scattering experiments of polymer blends generally involves assumptions about the randomness and homogeneity of the interface (or interphase), thereby making the entire analysis model dependent [9]. Bulky fluorescent labels may perturb their local environment altering the 10-Å short-range interactions over which they are generally used. None of these techniques is ideally suited, therefore, to the microscopic characterization of immiscible polymer-polymer interfaces and interphases which may vary in thickness from just a few Å to as much as 100 Å.

Cross-polarization, magic-angle spinning (CPMAS) ^{13}C nuclear magnetic resonance (NMR) has also been used to examine heterogeneous polymers [10]. For example, cross-polarization transfer from protons on chains in one phase to carbons of deuterated chains in another phase, has been used to establish the uniformity of the interphase in polystyrene-polybutadiene blends [11]. However, a heterogeneous cross-polarization transfer is a short-range probe of structure, and provides information about interchain distances no greater than 5 Å. This is the distance over which most *hetero*nuclear spins are effectively coupled.

For proton-rich polymers, *homo*nuclear proton spin exchange occurs readily and gives rise to the phenomenological description of proton-proton spin exchange as "spin diffusion" [12]. Spin diffusion (more accurately, polarization diffusion) is facile within a homogeneous phase and, in partially crystalline polymers, has been used to measure the

dimensions of domains of the order of 100 Å, [13-18] a distance much larger than that over which pairs of protons are strongly dipolar coupled.

Spin diffusion also crosses phase boundaries. McBrierty *et al* have explained the relaxation properties of the crystalline regions of a vinylidene fluoride-trifluoroethylene copolymer in terms of homonuclear spin diffusion from the amorphous regions into the crystalline regions [19,20]. In this situation, the rate of spin diffusion across a phase boundary and into the interfacial region depends on the geometry of the interface. Havens and VanderHart [21] have used the flux of polarization from one phase to another in partially crystalline poly(ethylene terephthalate) to determine crystallite surface areas and the effect of annealing on the crystallite surface to volume ratio. In both of these examples, successful detection of spin diffusion from one phase, across a phase boundary, and into the second phase, required either significant differences in the NMR relaxation properties of the two phases, or chemical-shift differences which permit inducing differences by special pulse sequences [22,23]. These differences allowed the polarization to be first "labeled" and then traced from one phase to the other [23,24].

Polymer Interfaces and Dynamic Nuclear Polarization: In this and the following three papers, we show that the characterization of the interfacial regions of immiscible polymer blends and composites of a variety of polymers, even non-crystalline polymers with quite similar ^{1}H chemical shift and relaxation properties, is possible using dynamic nuclear polarization (DNP) [25-29] with CPMAS ^{13}C NMR detection [30-32] of enhanced proton polarization. Stable free radicals are incorporated in just one of the components of a blend of two immiscible polymers. Proton

magnetization enhanced by dynamic nuclear polarization is generated in the undoped polymer phase by dipolar coupling to electrons in the doped polymer phase under microwave irradiation at the difference of the electron and proton Larmor frequencies. The larger magnetic moment of protons compared to that of carbons makes possible transfers from electrons to protons over greater distances than transfers from electrons to carbons. The enhanced proton polarization is then transferred to carbons under matched spin-lock Hartmann-Hahn [33] cross-polarization conditions [34] for detection with chemical-shift selectivity by magic-angle spinning [35,36] ^{13}C NMR with high-field proton decoupling [37]. Any carbon magnetization arising from chains in the undoped phase, which can be traced back to the pumping of the free radical, is necessarily an interface signal. The chains responsible for this signal will be between 10 and 100 Å from the free-radical source of magnetization regardless of whether the mechanism of polarization transfer across the interface was by H-H spin diffusion or by direct, long-range dipolar coupling of electrons to protons. This specificity can therefore be used to examine the structure and dynamics of polymer-blend interfaces directly and unambiguously.

The blends we have examined are immiscible mixtures of polycarbonate (PC) and polystyrene (PS) [38]. The PC/PS blend has the useful property of optical clarity because of an accidental matching of the refractive indices of the two homopolymers. If poly(styrene-acrylonitrile) copolymer replaces polystyrene, the resulting blend with polycarbonate is similar to commercial materials. Because the blend samples used in this work have interfaces rather than interphases, they should be considered as *models* for the commercial materials.

Selection of Parameters for Dynamic Nuclear Polarization: DNP-enhanced NMR has been used recently in studies of interfaces of semiconductor sandwiches [39]. These experiments are typically performed at low magnetic field and low temperature, on oriented crystals, having short electron and long nuclear spin-lattice relaxation times, and regular well-defined interfaces. Our samples are disordered glasses, having long electron and relatively short nuclear spin-lattice relaxation times, and highly irregular interfaces. These conditions dictate that we observe carbons rather than protons for chemical shift resolution, and so we perform the DNP experiment at high static magnetic field for efficient ^{13}C NMR detection. The high-field constraint makes impractical spin-locked electron-nuclear transfers [40-42]. Finally, because we are interested in the microscopic and macroscopic dynamic properties of the polymers as they are most commonly used, we perform our experiments near room temperature.

The polystyrene phase of our PC/PS blends are doped by bisdiphenylenephenylallyl free radical complex with benzene (BDPA). This free radical forms a homogeneous solid solution with both PC and PS [43]. The electrons are fixed in space (no molecular motion and no spin exchange) and have long electron spin-lattice relaxation times. Microwave irradiation under these conditions results in an enhanced proton polarization by the so-called "solid" effect [25,26] with no Overhauser enhancement [31]. Under favourable conditions, solid-effect DNP can enhance proton polarization by two orders of magnitude [29].

The results of our electron-proton-carbon DNP experiments on polymers and polymer blends are described in three papers (I-III). The first validates the observation of an interface signal; the second establishes

the mechanism of polarization transfer for this signal from the free-radical doped phase to the interface of the undoped phase; and the third paper describes the use of the signal to measure the molecular dynamics of chains in the interface. A fourth paper in this series (IV) describes our attempts to transfer polarization from electrons directly to carbons in polymers.

DYNAMIC NUCLEAR POLARIZATION BY THE SOLID EFFECT

Following Goldman [27], we consider an isolated electron (S) and nucleus (I), both spin one-half. The energy level diagram (Figure 1) connects transitions that are allowed ($\Delta m = \pm 1$) and forbidden ($\Delta m = 0,\pm 2$) *in zeroth order*. The pure spin-state character of all four levels is lost by the introduction of a pseudo-secular coupling, H_p, resulting in a Hamiltonian given by:

$$H = H_o + H_p \qquad (1)$$

$$H_o = \omega_I I_Z + \omega_S S_Z \qquad (2)$$

$$H_p = CS_Z I_+ + C^* S_Z I_- \qquad (3)$$

where H_o is the Zeeman Hamiltonian, ω_I and ω_S are Larmor frequencies, I_Z and S_Z are z-component angular-momentum spin operators for the nuclear and electron spins, respectively, C is the coupling parameter and the asterisk denotes complex conjugate. The nuclear-spin angular-momentum raising and lowering operators, I_+ and I_-, mix spin states. The extent of the mixing depends on the coupling parameter, C, where

$$C = \pm\frac{1}{2}D(3\cos^2\theta - 1) \qquad (4)$$

and $$D = \frac{\gamma_I \gamma_S h}{2\pi r^3} \qquad (5)$$

In the above equation, γ_I and γ_S are the I and S gyromagnetic ratios, h is Planck's constant, D is the dipolar coupling of the I and S spins, and r is the amplitude of the I-S internuclear vector which makes an angle, θ, with the applied static magnetic field.

Using first-order perturbation theory, we can write first-order corrections to the $\psi_k^{(o)}$ zeroth-order wavefunctions for the spin states,

$$\psi_n^{(1)} = \sum_{k \neq n} \psi_k^{(o)} \frac{V_{kn}}{E_n^\circ - E_k^\circ} \qquad (6)$$

where V_{kn} is the k,n matrix element of H_p. Using ket notation, the four spin states of Figure 2 are, to first order,

$$\begin{aligned} |a\rangle &= |{+}{+}\rangle + q^* |{+}{-}\rangle \\ |b\rangle &= |{+}{-}\rangle - q |{+}{+}\rangle \\ |c\rangle &= |{-}{+}\rangle - q^* |{-}{-}\rangle \\ |d\rangle &= |{-}{-}\rangle + q |{-}{+}\rangle \end{aligned} \qquad (7)$$

Thus, the energy of each of the mixed-spin states is shifted up or down by q (Figure 2), where

$$q = \frac{V_{kn}}{E_n^\circ - E_k^\circ} \qquad (8)$$

$$q = \frac{C}{2\omega_I} \qquad (9)$$

Because C measures dipolar coupling of a nucleus to an electron, q can be a sizable fraction of ω_I making transitions between all four states allowed.

The average transition probability between levels, W_{kn}, is given by the Fourier component of the autocorrelation of coupling to the applied radio or microwave-frequency field evaluated at the transition frequency. If W_o measures the probability of transitions between |a> and |c> and between |b> and |d>, then $W = W_o qq^*$ measures the probability of transitions between |a> and |d> and between |b> and |c>, transitions that were forbidden in zeroth order.

Using the average transition probability, we can write the coupled differential equations that describe the changes in electron and nuclear populations (and so polarizations) as a result of microwave irradiation at the difference of the electron and nuclear Larmor frequencies,

$$\frac{dP_I}{dt} = -N_S W(P_I - P_S) - \frac{1}{T_I}(P_I - P_I^\circ) \qquad (10)$$

$$\frac{dP_S}{dt} = -N_I W(P_S - P_I) - \frac{1}{T_S}(P_S - P_S^\circ) \qquad (11)$$

where N_I and N_S are the concentrations, P_I and P_S the polarizations, T_I and T_S the spin-lattice relaxation times, and P_I° and P_S° the equilibrium polarizations, of the nuclear and electron spins, respectively.

In steady state,

$$\frac{dP_I}{dt} = \frac{dP_S}{dt} = 0 \qquad (12)$$

and

$$P_I = \frac{P_I^\circ(1 + N_I W T_S) + P_S^\circ N_S W T_I}{1 + N_S W T_I + N_I W T_S} \qquad (13)$$

where $P_S^\circ >> P_I^\circ$. A similar analysis is possible for irradiation at the sum of electron and nuclear Larmor frequencies, in which case the P_S° term in the numerator of Equation (13) is negative. Thus, an enhanced nuclear polarization, P_I, of either sign, can be generated by microwave pumping of forbidden transitions if the multipliers of P_S° in Equation (13) are sizeable.

Dynamic nuclear polarization by the solid effect is illustrated in Figure 3. A single electron (big arrow) is dipolar coupled to many isolated nuclei (small arrows). The electron spin-lattice relaxation time T_S is much shorter than the nuclear spin-lattice relaxation time T_I. Thus, after a time of the order of T_I under microwave pumping, each electron is able to polarize many nuclei. Irradiation at the sum of the electron and nuclear Larmor frequencies induces "forbidden" double-quantum transitions leading to a negative DNP enhancement. Irradiation at the difference of the electron and nuclear Larmor frequencies produces a positive DNP enhancement by inducing "forbidden" zero-quantum, flip-flop, transitions. All of our DNP experiments were performed exclusively at the difference of the electron and proton Larmor frequencies.

The attempt to make the multipliers of P_S° large usually involves experimental compromises. High concentration of free radicals, strong electron-nuclear dipolar coupling, and intense microwave fields can lead to

large DNP enhancements, but at the price of NMR line broadening and sample heating which may not be acceptable. Reduction of the DNP enhancement (leakage) by multiple nuclear spin-lattice relaxation pathways (short T_1's) is always a factor. The theoretical maximum solid-effect enhancement for dipolar coupling between protons and electrons is 660. Experimental enhancements one or two orders of magnitude smaller are common.

EXPERIMENTS

The DNP Spectrometer: The DNP CPMAS ^{13}C NMR spectrometer operated at 39 GHz for electrons, 60 MHz for protons, and 15.1 MHz for carbons. The spectrometer was built around a horizontal six-inch bore Oxford super-conducting solenoid. The probe has all microwave components connected through one end of the magnet, and all radio-frequency (rf) components connected through the other. The microwave irradiation is down the axis of a cylindrical rf coil (Figure 4). The coil and a pneumatically operated reflector make up the microwave cavity. The magic-angle rotors have a hollowed T-shape configuration which allows placement of the waveguide within one mm of the spinning sample. The T-shape portion of the rotor is made of polyimide and the barrel that houses the sample is made of Kel-F and is rated for spinning speeds of up to 2 kHz. With this arrangement, there is no compromise in the inherent sensitivity of the ^{13}C rf channel. The CPMAS ^{13}C NMR spectra obtained with this spectrometer and another CPMAS spectrometer operating at about the same frequency were the same. Therefore, the microwave portion of the spectrometer does not, in

any way, degrade or otherwise alter the quality of the ^{13}C NMR spectra obtained.

All rf tuning components were external to the magnet [44]. ENI power amplifiers were used for both ^{1}H and ^{13}C channels. Two pulse programmer and data systems have been used, the first part of a Nicolet 1280 computer, interfaced to the spectrometer by a Hewlett-Packard terminal, and the second, a Tecmag pulse programmer controlled by a MacIntosh II microcomputer.

A high-voltage power supply from Universal Voltronics Corporation generated 3.17 kV and 80 ma to activate a Varian klystron that provided about 10 watts of microwave power at a frequency of 39 GHz. The frequency of the klystron was fixed and was measured by an EIP model 578 microwave source-locking counter. The static magnetic field was adjusted by an external Helmholtz coil and a dc power supply to match a resonance condition at the difference of the electron and proton Larmor frequencies.

Pulse Sequence: The DNP CPMAS ^{13}C NMR pulse sequence is shown in Figure 5. This is an alternate-block, add-subtract, equal-heat pulse sequence. This sequence was used to accumulate CPMAS ^{13}C signals whose origin can be traced back to microwave pumping of the unpaired electrons in the free-radical doped samples. In the first half of this experiment, samples are irradiated at the difference of the electron and proton Larmor frequencies for a period varying from 0.2 to 2.0 seconds. The microwave irradiation is followed by a standard CPMAS ^{13}C NMR pulse sequence. In the second half of the experiment, the CPMAS sequence is repeated with the microwave pumping delayed until after signal acquisition is completed.

Microwave pumping occurs during t_1, cross-polarization during t_2, and ^{13}C signal acquisition with proton dipolar decoupling during t_3. The $T_1(H)$ effects are equalized in the two halves of the experiment by inserting a delay equal to t_1 at the end of the first half. For samples with T_1 much shorter than the recycle delay, the t_1 delay for equalizing the T_1 effects of the two halves could be eliminated. The lower bound for t_1 is determined by $T_1(H)$, the rise time of the microwave field to full strength, and the time required to generate a DNP enhancement; the upper bound for t_1 is determined by microwave heating effects.

Thick Films of Homopolymers Doped with BDPA: The free radical used in all of the DNP experiments was a stable organic free radical called BDPA (1,3-bisdiphenylene-2-phenylallyl free-radical complex with benzene), purchased from Aldrich Chemical Company. The structure of BDPA is shown in Figure 6. Homopolymer samples of PC and PS with BDPA free radical as a dopant were prepared by dissolving a certain weight percent of BDPA and the homopolymer in chloroform. The resulting mixtures were stirred for uniform distribution of the free radicals. BDPA formed dilute solid, homogeneous solutions with PC and PS [43] as doped 1-mm thick films cast on glass plates from chloroform. Homopolymers homogeneously doped with BDPA were given the designations PC(*) and PS(*), the asterisk indicating the presence of BDPA in PC and PS, respectively.

At room temperature, the radical centers are fixed in space (no motion) and the unpaired electrons do not interact with each other resulting in T_{1e}'s of the order of a msec [45]. In this situation, sizeable DNP enhancements are achieved (Figure 7) even with modest microwave power by the solid effect, described in the previous section.

Thin-Film Blends of C-13 Enriched PC and C-13 Depleted or Perdeuterated PS with BDPA: Homopolymer solutions were prepared by dissolving 174 mg PC(^{13}C) in chloroform at 25 °C, and 180 mg PS(^{12}C) or PS(^{2}D) with 4 mg BDPA in cyclohexane at 38 °C. The solutions were 1% by weight polymer in their respective solvents. The concentration of BDPA in each of the PS solutions was 2% by weight. A microscope glass slide was dipped into the PC-chloroform solution for about five seconds, and the solvent allowed to evaporate in air for about an hour leaving a thin film of PC. Then the same glass slide that already had a PC film was dipped into the cyclohexane solution of PS and BDPA. Cyclohexane is not a solvent for PC, so the PC film that was on the glass slide was not obviously affected by the second dipping. Thus a thin film of PS with BDPA was layered on top of the PC film (Figure 8). This serial film casting was repeated with about 100 microscope glass slides to obtain enough sample for NMR experiments. The sandwich films were dried in a vacuum oven at 50 °C for about 20 hours. The central, uniform portions of the sandwich films were then scraped from the slides using a razor blade. About 1.6 mg of blend sample was recovered from each glass slide. From the weight recovered from the slides, the area of the glass slide, and the density of the polymers, the thickness of the sandwich films was estimated to be 0.6 μ (microns). A total of 133 mg and 138 mg of two blend samples, denoted by PC(^{13}C)/PS(^{12}C/*) and PC(^{13}C)/PS(^{2}D/*), respectively, were pressed at 500 psi at room temperature to make pellets for the magic-angle rotor. As with the homopolymer-BDPA samples, the asterisk within parentheses indicates the presence of homogeneously dispersed BDPA in either the ^{13}C-depleted or perdeuterated PS phase; the

slash outside of the parentheses indicates some sort of interface between the PC and PS polymers.

C-13 enriched PC and BDPA: A serial film casting was made first from a PC-chloroform solution and then, after drying the glass slides in air for about an hour, from a BDPA-cyclohexane solution at 38 °C. In this case the BDPA for the most part appeared to have crystallized on top of the PC film. The films were scraped from the glass slides using a razor blade. A 76-mg sample was recovered for NMR experiments, and given the designation PC(^{13}C)/*. Here the slash is an indication of the fact that the BDPA was not homogeneously distributed throughout the PC phase.

All of these samples were stored at room temperature and 40% relative humidity. Once the samples were pressed into pellets they remained in that form throughout the duration of this work. They were stable and could be used again and again with reproducible results under normal experimental conditions.

RESULTS

DNP of Homopolymers: After 1.0-second microwave irradiation, and a transfer of polarization from protons to carbons by a 2.0-ms cross-polarization contact at 50 kHz, the DNP enhanced CPMAS ^{13}C NMR spectrum of PS(*) is a factor of 20 more intense than that of a conventional CPMAS spectrum (Figure 9). Higher enhancements were achieved with 4% free radical doping but the resultant ^{13}C lineshapes were broadened (data not shown).

The standard CPMAS ^{13}C NMR spectra of the labeled polymers are shown in Figure 10. The PC sample was labeled at ring positions 3 and 3' with 99 atom % ^{13}C; all the other carbon atoms were at the natural-abundance ^{13}C level. The PS sample was ^{13}C depleted in all phenyl-ring carbon atoms which were at least 99.97 atom % ^{12}C enriched. The aliphatic carbons were at the natural-abundance ^{13}C level. The protonated, aromatic-carbon resonance of the labeled PC sample is at δ_C 120 (Figure 10, bottom) and the residual ring-^{13}C resonance of the depleted PS is at δ_C 125 (Figure 10, top). The labeled, protonated, aromatic-carbon peak of PC is distinct from the residual aromatic-carbon PS peak.

Interface-PC Signal Detection: Normal CPMAS ^{13}C NMR signals in bulk PC homopolymers are cancelled exactly (Figure 11) by the alternate-block, add-subtract, equal-heat pulse sequence of Figure 5, using microwave irradiation for 1.0 second, matched H-C cross-polarization at 50 kHz for 1 ms, and ^{13}C signal acquisition for 25 ms with H-C dipolar-decoupling fields at 80 kHz. A DNP enhancement is observed, however, for both PC and PS components of a thin-film blend of PC(^{13}C) and BDPA-doped PS(^{12}C), the blend sample designated as PC(^{13}C)/PS(^{12}C/*). In the DNP-enhanced spectrum (Figure 12, bottom), the aliphatic-carbon peak of PS at δ_C 45 is clearly enhanced relative to that of the standard CPMAS ^{13}C NMR spectrum (Figure 12, middle). The peaks at δ_C 0 and 245 are spinning sidebands. Although not immediately obvious, the protonated aromatic-carbon peak of labeled PC is also enhanced. The difference spectrum shown at the top of the figure (bottom minus middle) shows a contribution from PC at δ_C 120. This signal has about one-fifth of the intensity of the ^{13}C natural-abundance aliphatic-carbon signal of bulk PS (δ_C 45), and is 4% of the

intensity of the bulk protonated aromatic-carbon signal in an ordinary CPMAS ^{13}C NMR experiment on the same sample. A minor contribution to the DNP difference spectrum is also observed from the residual ^{13}C atoms of the ^{13}C-depleted PS aromatic-carbons of the phenyl ring; this is the shoulder at δ_C 125 in Figure 12 (top). No difference signal is observed for PC(^{13}C)/* (Figure 13).

The alternate-block, DNP difference experiment was performed at both high and low microwave power. Lower microwave power (about 50% of maximum) avoids ^{13}C line broadening (Figure 14, bottom) but reduces the PS aliphatic-carbon enhancement to about half the maximum value. The origin of broadened DNP-difference peaks at higher microwave power will be discussed in III and IV.

DISCUSSION

Interface NMR Signals: Strictly speaking, the observation of the PC signal by the DNP-difference experiment on the thin-film blend (δ_C 120, Figure 12, top) is not necessarily a detection of chains at the interface of the PC/PS blend. A free-radical leakage from the BDPA-doped PS phase to the PC phase would give similar results. However, the absence of an enhanced signal for PC(^{13}C)/* demonstrates that there is no free-radical penetration of the thin PC film in PC(^{13}C)/*. This implies the absence of BDPA in the PC phase of the thin-film blend PC(^{13}C)/PS(^{12}C/*). We conclude that the PC signal in the DNP-difference experiment is indeed from PC chains *at the interface*. For PC(^{13}C)/* there was no penetration of the PC film by the free radicals and hence no contact of PC chains with BDPA on a molecular level.

On drying, BDPA simply formed crystals on the film surface. Physically mixing BDPA and polymer powders also never resulted in a DNP difference signal. For DNP enhancements, the free radicals must be molecularly dispersed in the polymer chains.

Thin-Film Blends: The serial film casting on microscope glass slides used to make the thin-film blends of ^{13}C-enriched PC and BDPA-doped ^{13}C-depleted PS guarantees exclusion of the free radicals from one component of the blend. The method is general, assuming the appropriate solvent and nonsolvent pair can be found for the two polymer components of the immiscible blend. In addition, the extent of microscopic contact between the two phases is known, at least semiquantitatively, from the weight of the blend, the densities of the two components, and the surface area of the glass-slide. However, the films are not particularly uniform (±10%) and not much film is produced per microscope slide. Casting multilayer sandwiches on microscope slides to produce more material (and also to increase the interfacial volume fraction) makes even less uniform films. It is possible to generate more uniform thin-film polymer blends by serial spin coating an optically flat silicon wafer, but this approach is not practical with expensive, labeled polymers because of the difficulty of recovery of material spun off the rotating wafer disk. The problem of limited contact between polymer components can be solved by covalently attaching a stable free radical to one of the polymers. (As discussed earlier, the ESR properties of the free radical are crucial to a successful DNP experiment; in particular, large hyperfine splittings must be avoided.) Then blends with high interphase volume fractions can be formed by coprecipitation or by film casting from a common solvent.

Electron-Nuclear Polarization Transfer: We have been unable to detect a direct DNP transfer from *electrons* in PS to *carbons* in PC in thin-film blends (data not shown). This can be explained by a combination of distance effects and lower sensitivity. The electron-carbon coupling is not as strong as the electron-proton coupling due to the lower gyromagnetic ratio for carbons. A direct DNP transfer from electrons to PC carbons is therefore limited to carbons closer to the interfacial boundary than for the corresponding PC protons. Carbons with strong enough dipolar coupling to electrons to be enhanced by DNP will have resonances shifted in frequency thereby resulting in line broadening. In addition, mobile carbons in PC that are close to electrons will have a short T_1(C) making polarization build up difficult. Nevertheless, direct electron-to-carbon polarization transfers have been observed for PC(*) and PC(^{13}C/*), where the mixing of the free radicals and the polymer was done homogeneously. These experiments will be described in IV.

The PC interface signal of Figure 12 was obtained by a double polarization transfer: electrons to protons to carbons. The double-transfer approach is essential in generating an interfacial PC signal in these thin-film polymer blends. We discuss in the following paper whether this transfer is from electrons to PS protons or from electrons to PC protons, over what distances the transfers were made, and the extent of spin diffusion of the enhanced polarization among the protons prior to the transfer to carbons.

ACKNOWLEDGEMENTS

The magic-angle spinning device illustrated in Figure 4 was designed and built by E.O. Stejskal (North Carolina State University, Raleigh) at the Monsanto Company in 1984-85. The DNP spectrometer was donated by Monsanto Company to Washington University in 1986. The ^{13}C-labeled polycarbonate was synthesized by S. Bales (Dow Chemical Company, Midland) and the ^{13}C-depleted polystyrene was synthesized by A.R. Padwa (Monsanto Company, Springfield). This work has been supported by the Office of Naval Research under contract N00014-88-K-0183.

REFERENCES

1. Paul, D.R. *Adv. Chem.*, **1986**, *211*, 3.
2. MacKnight, W.J.; Karasz, F.E.; Fried, J.R. in *Polymer Blends*, Vol.1, Academic Press, New York, **1978**, p. 185.
3. Utracki, L.A. in *Polymer Alloys and Blends: Thermodynamics and Rheology*, Oxford Univ. Press, New York, **1990**, p. 118 (and references therein).
4. Fried, J.R. in *Developments in Polymer Characterization*, Appl. Sci., London, **1983**, p. 39.
5. Manson, J.A.; Sperling, L.H. *Polymer Blends and Composites*, Plenum Press, New York, **1976**, p. 109.
6. Higgins, J.; Stein, R.S. *J. Appl. Crystallogr.*, **1978**, *11*, 346.
7. Wignall, C.D.; Child, H.R.; Li-Aravena, F. *Polymer*, **1980**, *17*, 640.
8. Amrani, F.; Hung, J.M.; Morawetz, *Macromolecules*, **1980**, *13*, 649.
9. Schaefer, J.; Garbow, J.R.; Stejskal, E.O.; Lefelar, J.A. *Macromolecules*, **1987**, *20*, 1271.
10. Stejskal, E.O.; Schaefer, J.; Sefcik, M.D.; McKay, R.A. *Macromolecules*, **1981**, *14*, 275.
11. Schaefer, J.; Sefcik, M.D.; Stejskal, E.O.; McKay, R.A. *Macromolecules*, **1981**, *14*, 188.
12. Abragam, A. in *The Principles of Nuclear Magnetism*, Chap. V, Oxford Univ. Press, London, **1961**.
13. Goldman, M.; Shen, L. *Phys. Rev.*, **1966**, *144*, 321.
14. Cheung, T.T.P.; Gerstein, B.C. *J. Appl. Phys.*, **1981**, *52*, 5517.
15. Assink, R.A. *Macromolecules*, **1978**, *11*, 1233.

15. Assink, R.A. *Macromolecules*, **1978**, *11*, 1233.

16. Cheung, T.T.P.; Gerstein, B.C.; Ryan, L.M.; Taylor, R.E.; Dybowski, C.R. *J. Chem. Phys.*, **1980**, *73*, 6059.

17. Packer, K.J.; Pope, J.M.; Yeung, R.R.; Cudby, M.E.A. *J. Polym. Sci. Polym. Phys. Ed.*, **1984**, *22*, 589.

18. McBriety, V.J.; Douglass, D.C.; Kwei, T.K. *Macromolecules*, **1978**, *11*, 1265.

19. McBriety, V.J.; Douglass, D.C. *Phys. Rev.*, **1980**, *63*, 61.

20. McBriety, V.J.; Douglass, D.C. *Macromol. Rev.*, **1981**, *16*, 295.

21. Havens, J.R.; VanderHart, D.L. *Macromolecules*, **1985**, *18*, 1663.

22. Campbell, G.C.; VanderHart, D.L. in *Tailoring of Polarization Gradients for Studying Chemically Similar Polymer Blends via Proton Spin Diffusion*, poster at the 31st Experimental NMR Conference, Asilomar, April, **1990**.

23. Schmidt-Rohr, K.; Clauss, J.; Blumich, B.; Spiess, H.W.; *Mag. Reson. Chem.*, **1990**, *28*, 53.

24. Caravatti, P.; Neuenschwander, P.; Ernst, R.R. *Macromolecules*, **1985**, *18*, 119; **1986**, *19*, 1889.

25. Abragam, A.; Proctor, W.G. *C.R. Acad. Sci.*, **1958**, *246*, 1258.

26. Borghini, M.; Abragam, A. *C.R. Acad. Sci.*, **1959**, *248*, 1803.

27. Goldman, M. in *Spin Temperature and Nuclear Magnetic Resonance in Solids*, Clarendon Press, Oxford, **1970**, p. 178.

28. Hausser, K.H.; Stehlik, D. *Adv. Magn. Reson.*, **1968**, *3*, 79.

29. Brunner, H.; Hausser, K.H.; Keller, H.J.; Schweitzer, D. *Solid State Comm.*, **1984**, *51*, 107.

30. Wind, R.A.; Duijvestijn, A.; van der Lugt, C.; Manenschijn, A.; Vriend, J. *Prog. in NMR Spectrosc.*, **1985**, *17*, 33.

31. Overhauser, A.W. *Phys. Rev.*, **1953**, *92*, 411.

32. Duijvestijn, A.; Manenschijn, A.; Smidt, J.; Wind, R.A. *J. Magn. Reson.*, **1985**, *64*, 461.

33. Hartmann, S.; Hahn, E.L. *Phys. Rev.*, **1962**, *128*, 2042.

34. Pines, A.; Gibby, M.G.; Waugh, J.S. *J. Chem. Phys.*, **1973**, *59*, 569.

35. Lowe, I.J. *Phys. Rev. Letters*, **1959**, *2*, 285.

36. Andrew, E.R.; Bradbury, A.; Eades, R.G. *Nature* (London), **1958**, *182*, 1659.

37. Bloch, F. *Phys. Rev.*, **1958**, *111*, 841.

38. Peterson, R.J.; Corneliussen, R.D.; Rozelle, L.T., *Polym. Prepr. Amer. Chem. Soc. Div. Polym. Chem.*, **1969**, *10*, 385.

39. Denninger, G. *Advances in Solid-State Physics*, **1990**, *30*, 13.

40. Henstra, A.; Dirksen, P.; Schmidt, J.; Wenckebach, W.Th., *J. Magn. Reson.* **1988**, *77*, 389.

41. Henstra, A.; Dirksen, P.; Wenckebach, W.Th., *Phys. Lett. A*, **1988**, *134*, 144.

42. Henstra, A.; Lin, T.-S.; Schmidt, J.; Wenckebach, W.Th., *Chem. Phys. Lett.* **1990**, *165*, 6.

43. Goldsborough, J.P.; Mandel, M.; Pake, G.E. *Phys. Rev. Lett.*, **1960**, *4*, 13.

44. McKay, R.A., U.S. Patent 4,446,431 (May 1, 1984).

45. Hans Thomann (Exxon Research and Engineering Company), private communication.

FIGURE CAPTIONS

Figure 1. Energy-level diagram of uncoupled electron (S) and nuclear (I) spins in a strong external magnetic field. The solid lines indicate the ESR (ω_S) and NMR (ω_I) transitions corresponding to $\Delta m = \pm 1$; these are allowed transitions. The dashed lines indicate the zeroth-order "forbidden" transitions corresponding to $\Delta m = 0, \pm 2$. The four energy levels are labeled by M_S, M_I.

Figure 2. Energy-level diagram of an electron and nuclear spin pair with dipolar coupling. The spin states are identified in Equation (7) of the text.

Figure 3. A single electron (big arrow) is dipolar coupled to many isolated nuclei (small arrows). Irradiation at the sum of the electron (S) and nuclear (I) Larmor frequencies induces "forbidden" double-quantum transitions leading to a negative DNP enhancement. The electron spin-lattice relaxation time (T_S) is short while the nuclear spin-lattice relaxation times (T_I) are long. Thus, a single electron can polarize many nuclei under microwave pumping. Irradiation at the difference of the electron and nuclear Larmor frequencies produces a positive DNP enhancement by inducing "forbidden" zero-quantum, flip-flop transitions.

Figure 4. Rotor, stator, radio-frequency (rf) coil, and waveguide configuration of the DNP CPMAS ^{13}C NMR spectrometer. Remote rf tuning elements are connected to the coil by a transmission line (not shown in the figure). The movable plunger (reflector) is pneumatically operated and

together with the rf coil makes up the microwave cavity. The magic angle, β, is 54.7°.

Figure 5. Pulse sequence for DNP-enhanced CPMAS ^{13}C NMR. Microwave pumping occurs during t_1, cross-polarization during t_2, and ^{13}C acquisition with H-C dipolar decoupling and magic-angle spinning occurs during t_3. One block of the add-subtract, equal-heat, alternate-block sequence has the microwave irradiation after data acquisition has been completed. Relaxation effects during the two halves are equalized by inserting a t_1 delay at the end of the first half. Ordinary CPMAS ^{13}C NMR signals cancel exactly, so any difference signal obtained is from carbons coupled to electrons via the protons.

Figure 6. Structure of 1,3-bisdiphenylene-2-phenylallyl (BDPA) free-radical complex with benzene.

Figure 7. Inverse of the proton-observed DNP enhancements in PS(*) and PC(*) as a function of the inverse of the relative microwave-irradiation power. The inverse enhancements are expressed as $\frac{I_o}{I-I_o}$, where I is the integrated intensity of the solid-echo signal with microwave irradiation and I_o without microwave irradiation. The enhancements at infinite microwave power are obtained by extrapolation.

Figure 8. Preparation of a thin film of polycarbonate-polystyrene blend by double casting. The PC was cast from chloroform solution and the PS with BDPA from a solution of cyclohexane at 38 °C. The asterisk within

parentheses indicates the presence of homogeneously-dispersed free radicals in the PS phase.

Figure 9. 15.1-MHz CPMAS ^{13}C NMR spectra of BDPA-doped polystyrene with (bottom) and without (top) 1.0-second microwave irradiation at the difference of the electron and proton Larmor frequencies. The microwave irradiation produces a positive DNP enhancement. The peak around δ_C 40 is from the aliphatic carbons, the peak around δ_C 125 is from all protonated, aromatic carbons, and the peak around δ_C 145 is from the non-protonated aromatic carbon.

Figure 10. 15.1-MHz CPMAS ^{13}C NMR spectra of ^{12}C-enriched (99.97 atom %) polystyrene, PS(^{12}C), (top) and ^{13}C-enriched (99 atom %)polycarbonate, PC(^{13}C), (bottom). A total of 15,000 and 2760 scans were averaged to generate the PS and PC CPMAS spectra, respectively. Matched spin-lock transfers were made in 1.0 ms at 40 kHz; 80-kHz dipolar-decoupling fields were used. Spinning sidebands are designated "ssb".

Figure 11. 15.1-MHz CPMAS ^{13}C NMR spectra of PC(^{13}C) with (bottom) and without (middle) 1.0-second microwave irradiation. A total of 2475 scans were averaged to obtain each spectrum. The null spectrum shown at the top is the difference (bottom minus middle).

Figure 12. 15.1-MHz CPMAS ^{13}C NMR spectra of PC(^{13}C)/PS(^{12}C/*) with (bottom) and without (middle) 1.0-second microwave irradiation. The difference spectrum (top) has a polycarbonate contribution (δ_C 120) arising

from PC chains at the interface. Each spectrum was generated by 72,000 scans with a 1.0-second recycle period.

Figure 13. 15.1-MHz CPMAS ^{13}C NMR spectra of a thin film of PC(^{13}C)/*. A thin-film PC(^{13}C) on a microscope glass slide was dipped in a cyclohexane solution of BDPA at 38 °C (with no polystyrene present in the cyclohexane solution) and then dried. The BDPA crystallized on the surface of the polycarbonate film. The linewidth increase is due to bulk-susceptibility broadening. The spectra were obtained by a CPMAS ^{13}C NMR with (bottom) and without (middle) 1.0-second microwave irradiation. About 5000 scans were averaged to obtain each spectrum. The difference spectrum is shown at the top of the figure, a null indicating that the BDPA has not penetrated the chains of polycarbonate.

Figure 14. 15.1-MHz CPMAS ^{13}C NMR DNP difference spectra of the thin-film PC(^{13}C)/PS(^{12}C/*) blend. Increasing microwave power increases the difference signal intensity but broadens the lines (top spectrum) because of contributions from carbons that are close to the free-radical centers. In both cases 1.0-second microwave irradiation was used. The spectrum at the top of the figure is an expanded version of the spectrum shown in Figure 12 (top).

Figure 1

Figure 2

$$q = \frac{V_{kn}}{E_n^o - E_k^o} \qquad = \frac{C}{2\omega_I}$$

Figure 3

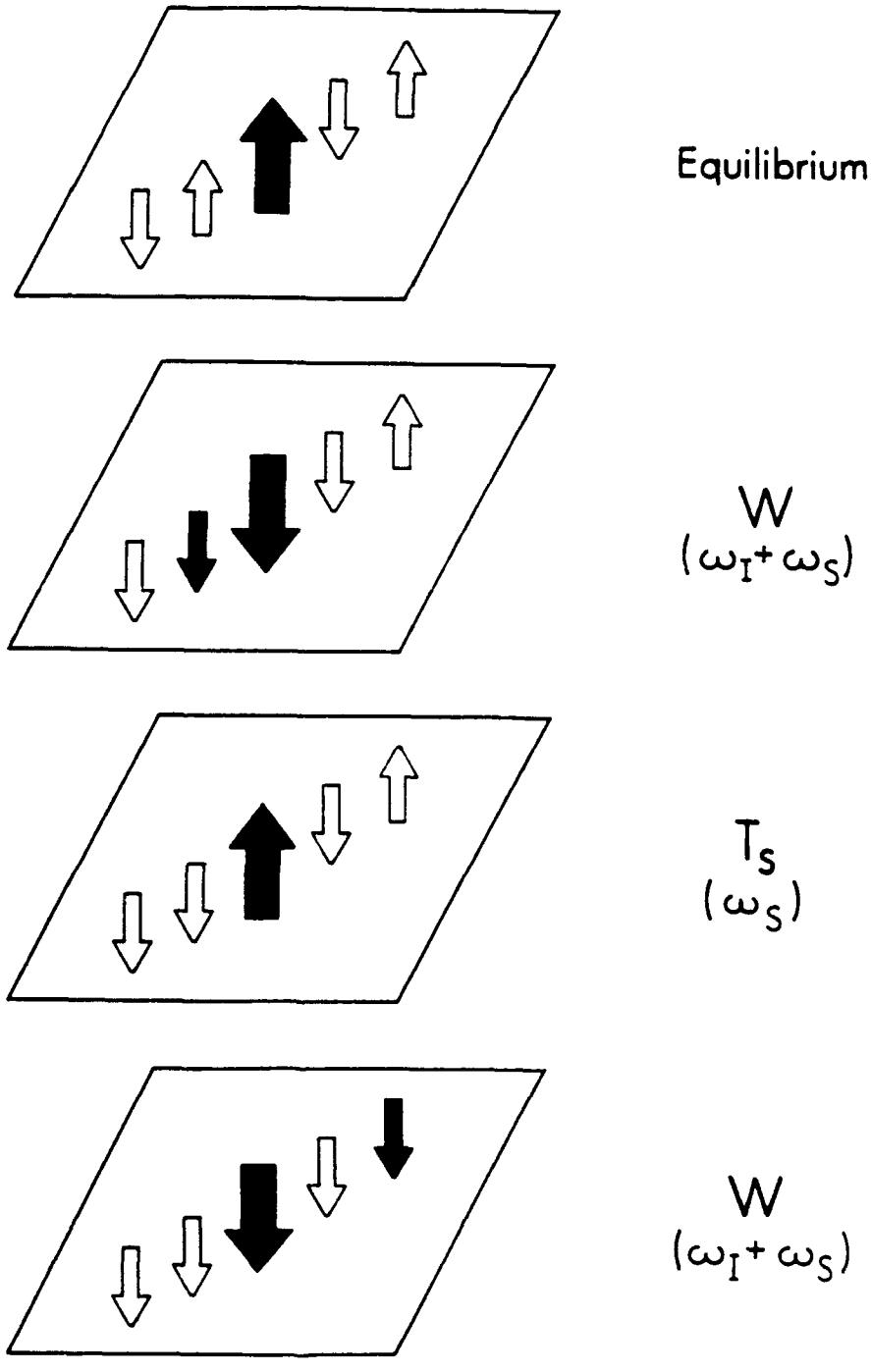

Figure 4

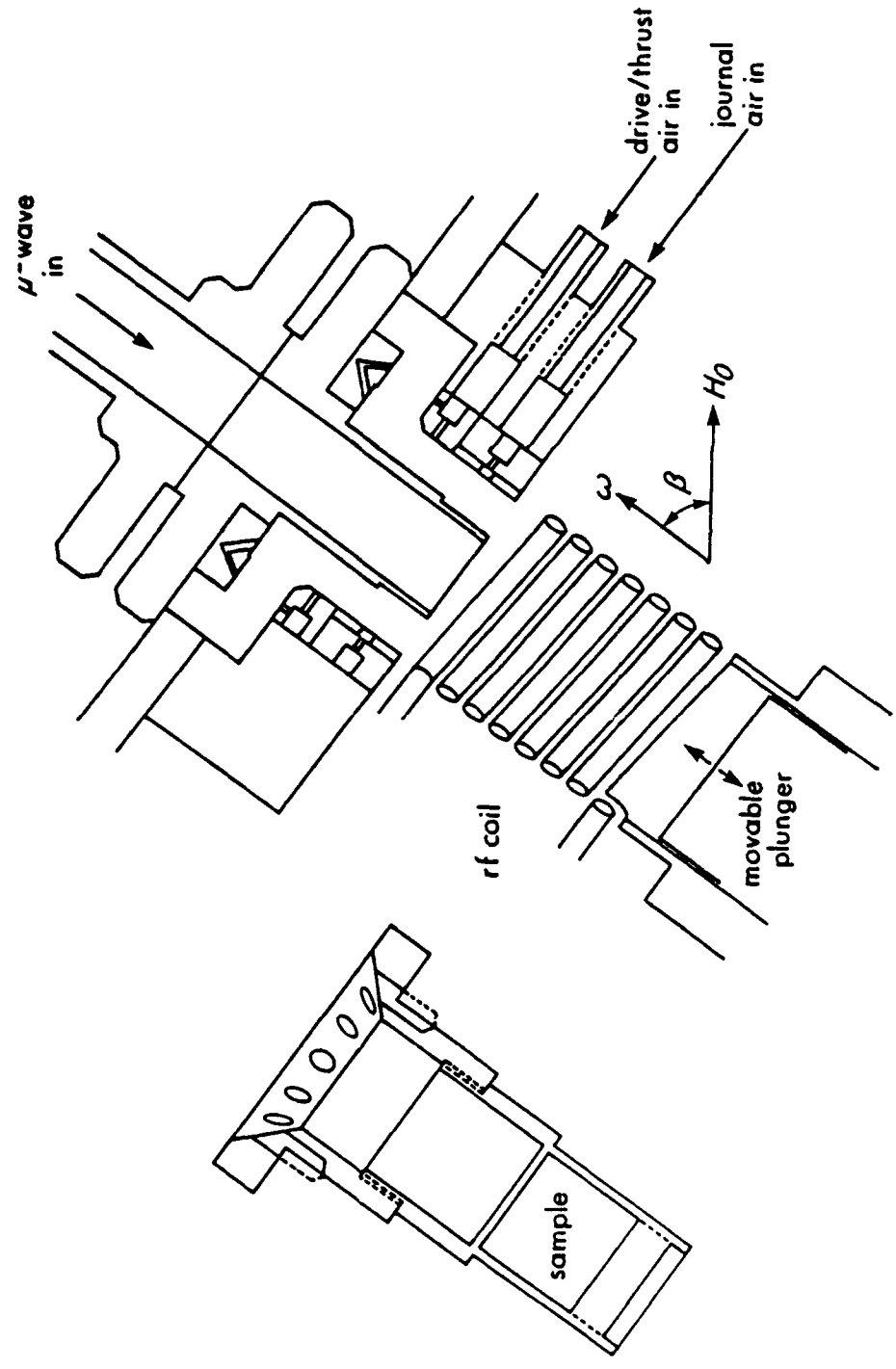
drive/thrust air in
journal air in
μ-wave in
H_0
ω
β
rf coil
movable plunger
sample

Figure 5

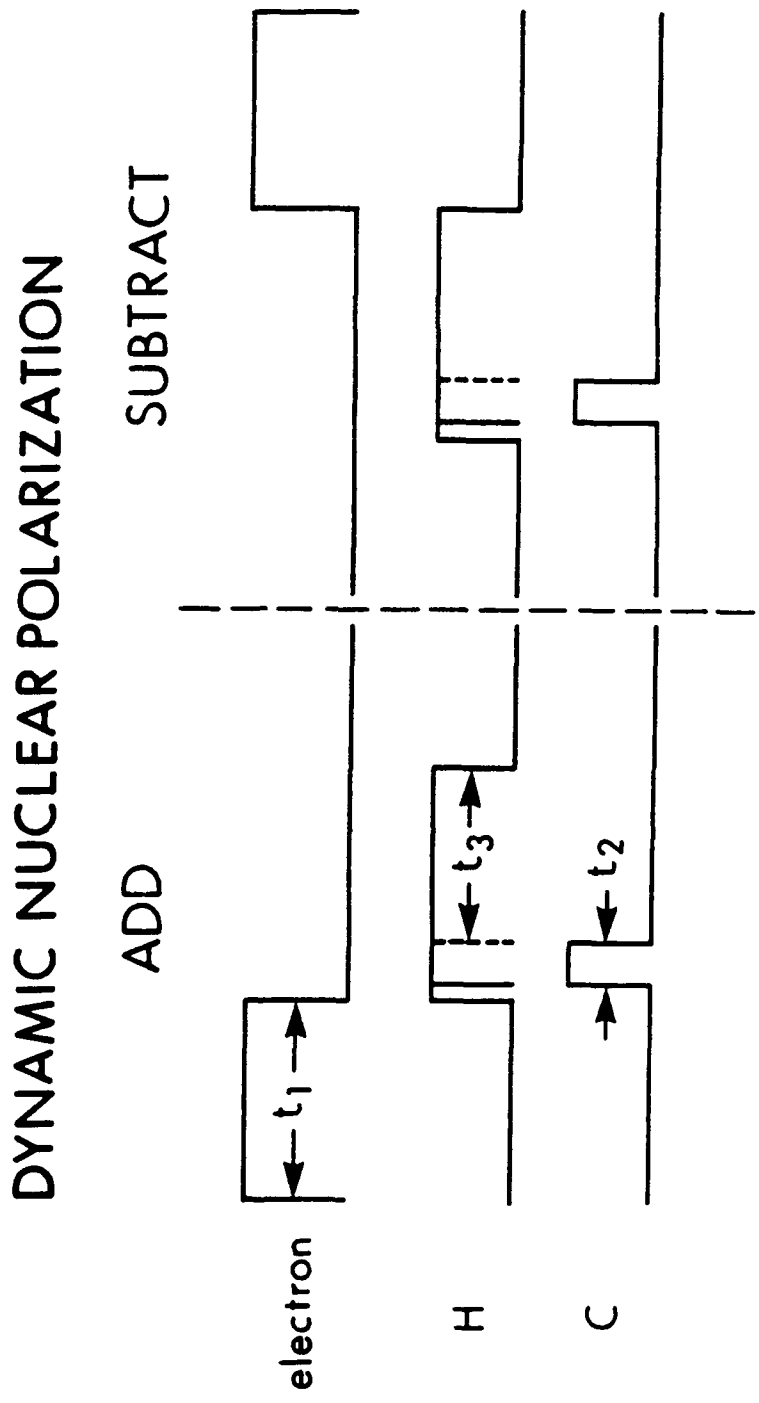
DYNAMIC NUCLEAR POLARIZATION
ADD
SUBTRACT
t_1
t_3
t_2
electron
H
C

Figure 6

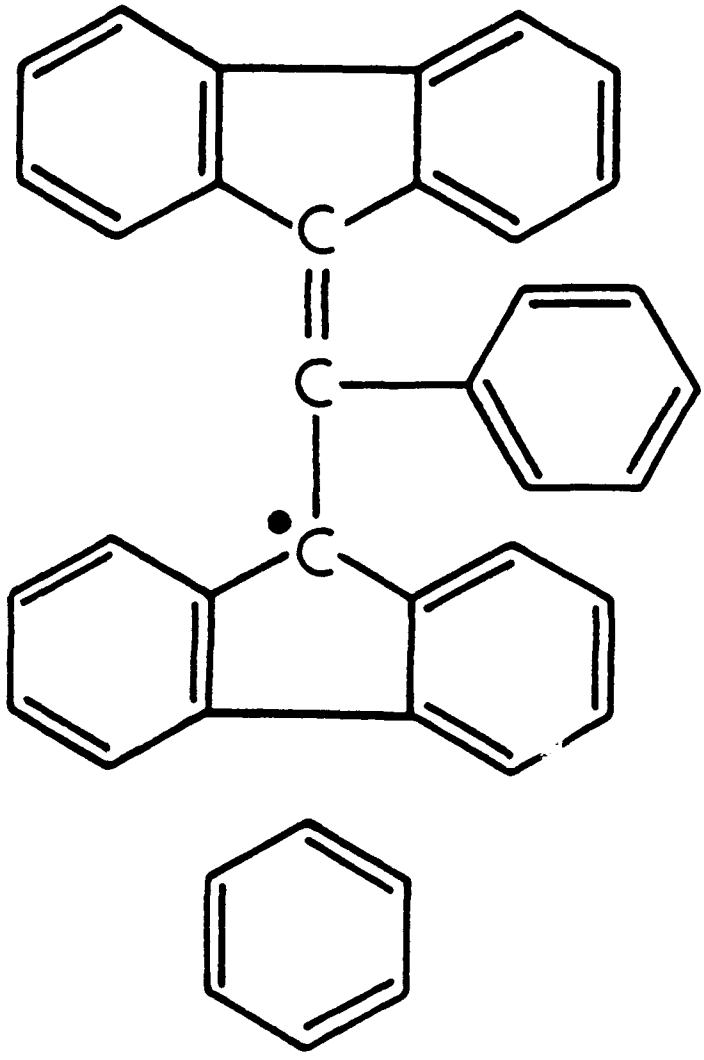

α,γ - bisdiphenylene - β - phenylallyl
free - radical complex with benzene

Figure 7

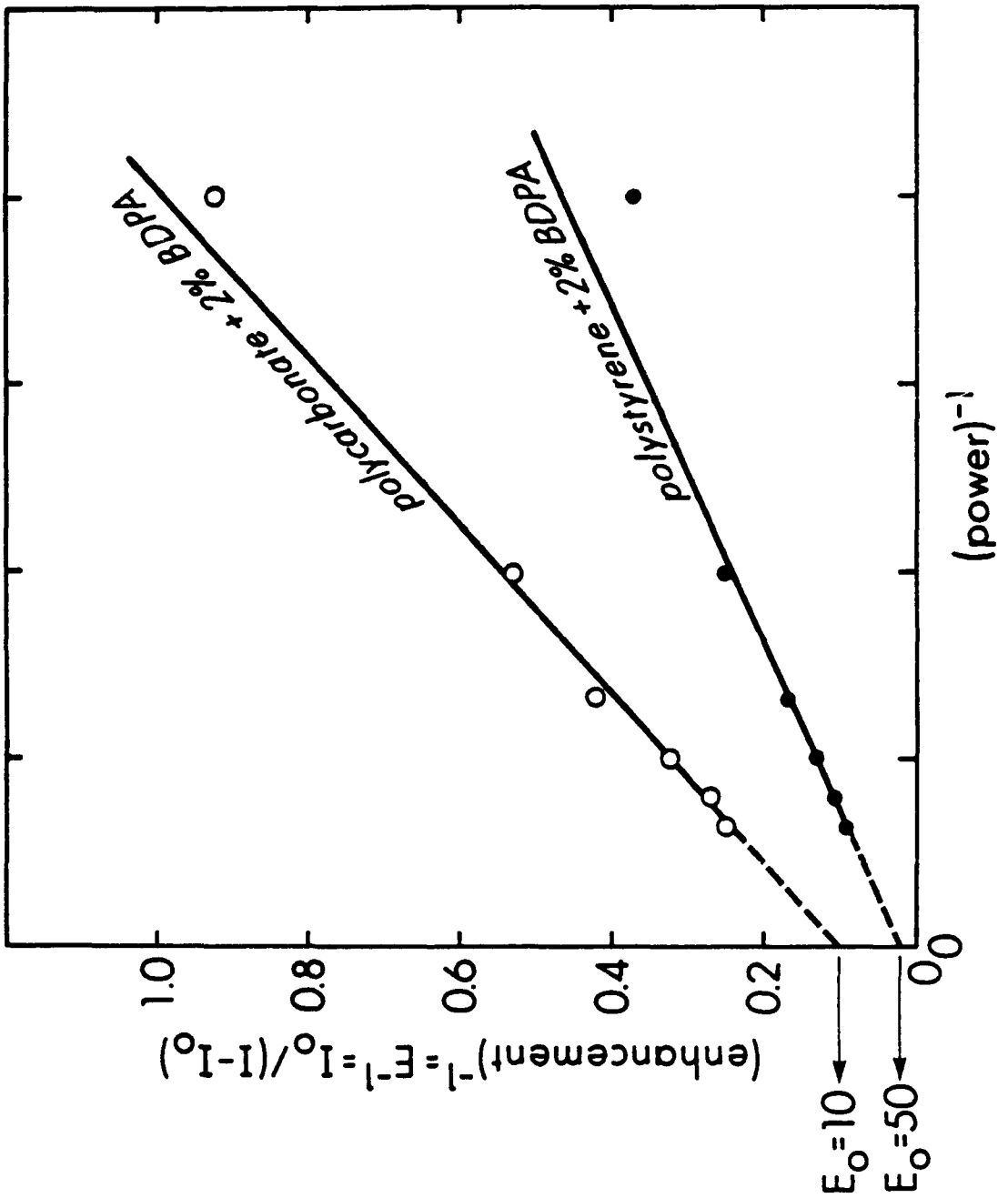
polystyrene + 2% BDPA
polycarbonate + 2% BDPA
(enhancement)$^{-1}$ = $E^{-1} = I_o/(I-I_o)$
(power)$^{-1}$
1.0
0.8
0.6
0.4
0.2
0
E_o=10
E_o=50

THIN-FILM PREPARATION

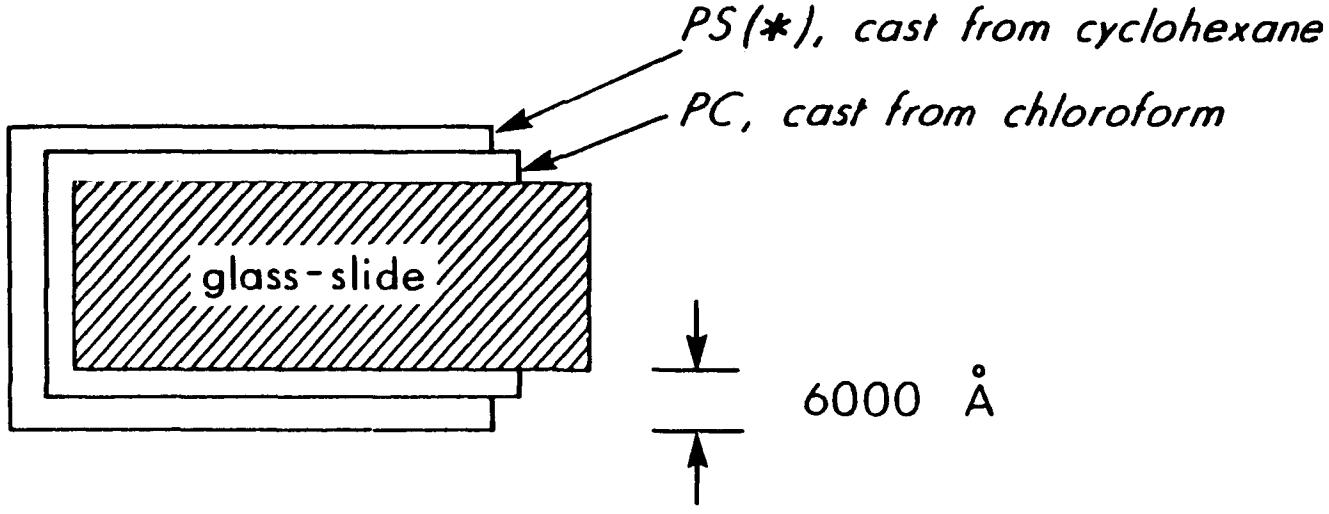

Figure 8

Figure 9

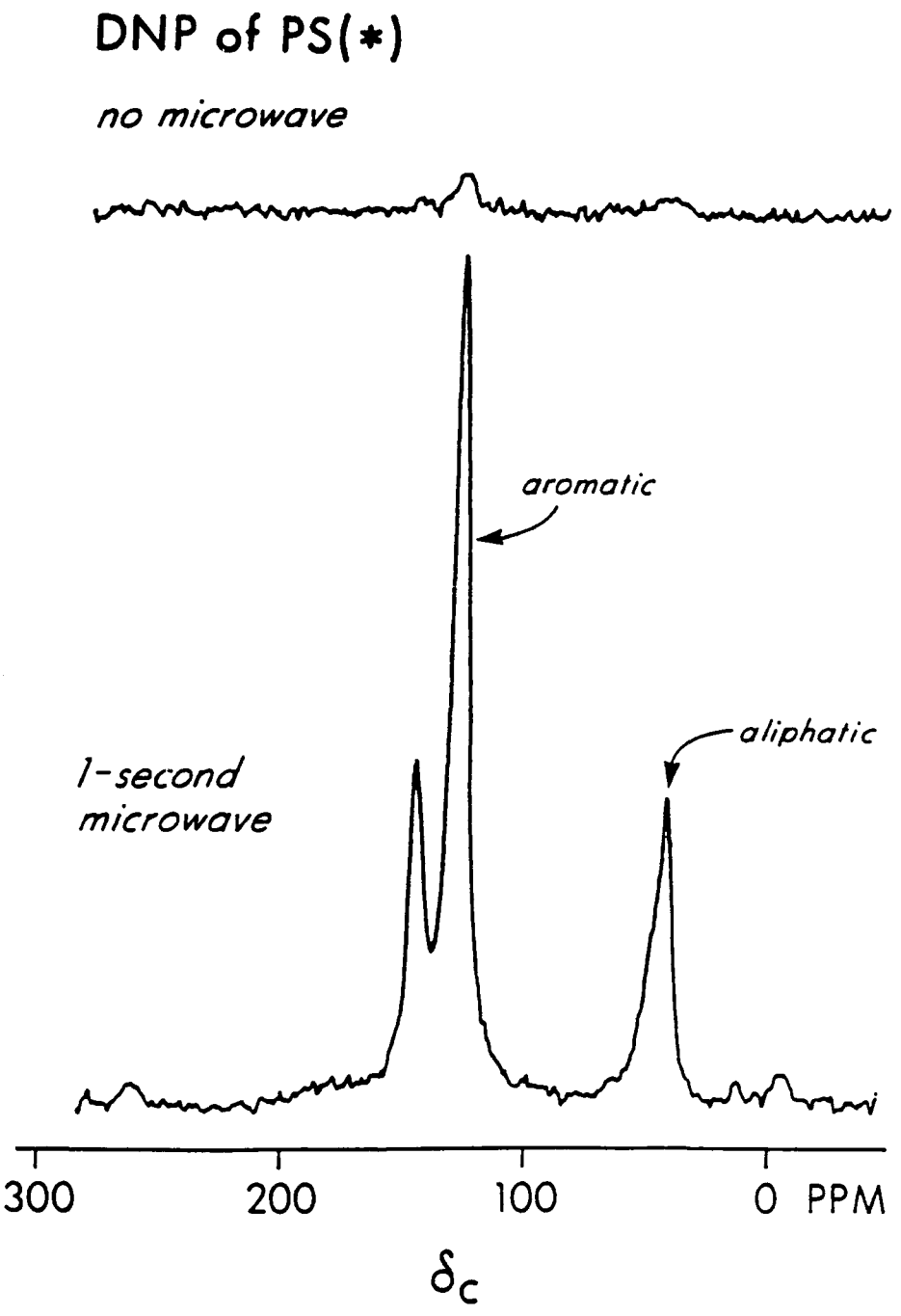
DNP of PS(*)
no microwave
aromatic
aliphatic
1-second
microwave
300
200
100
0 PPM
δC

Figure 10

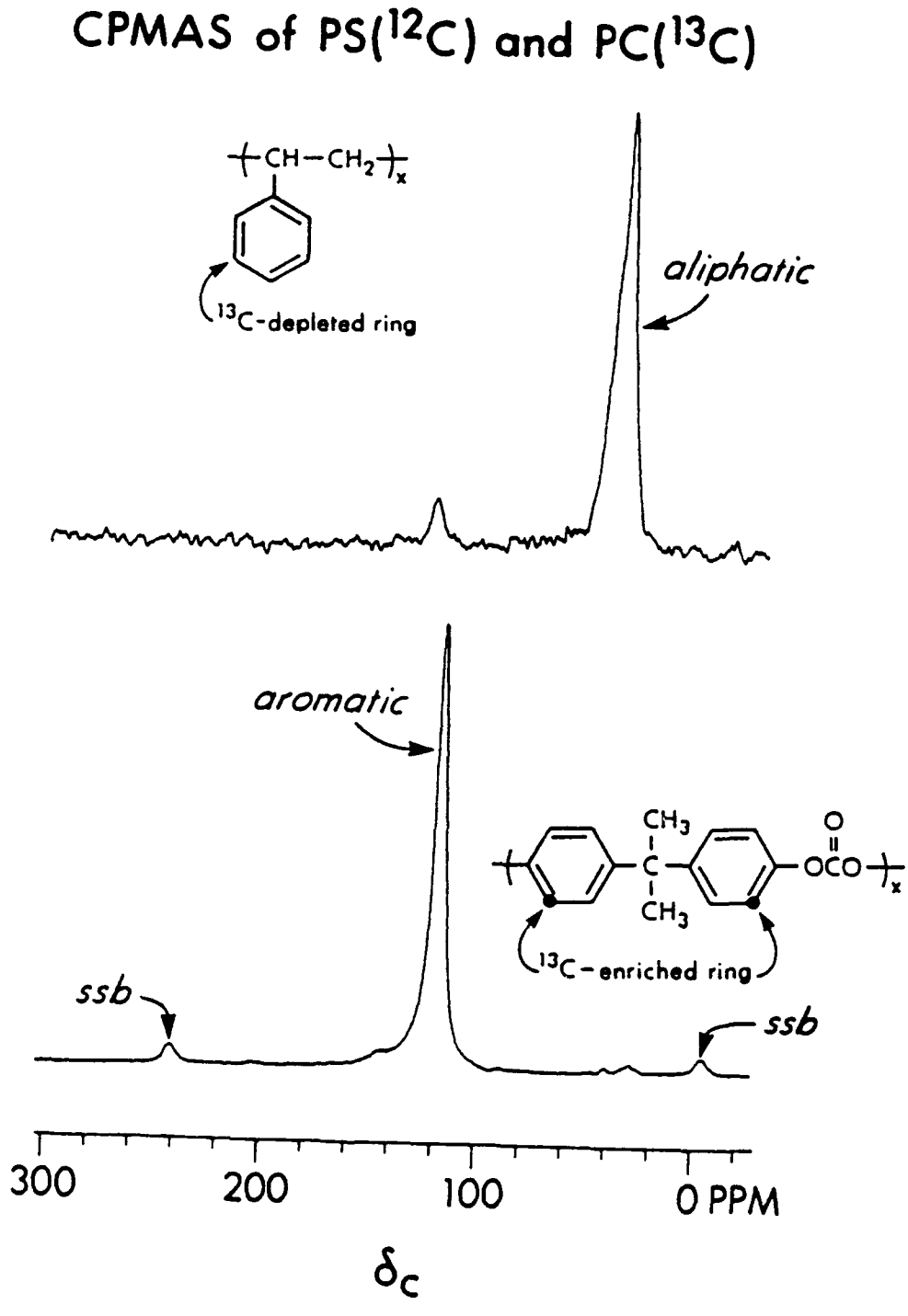
CPMAS of PS(^{12}C) and PC(^{13}C)
^{13}C-depleted ring
aliphatic
aromatic
^{13}C-enriched ring
ssb
ssb
300
200
100
0 PPM
δ_C

Figure 11

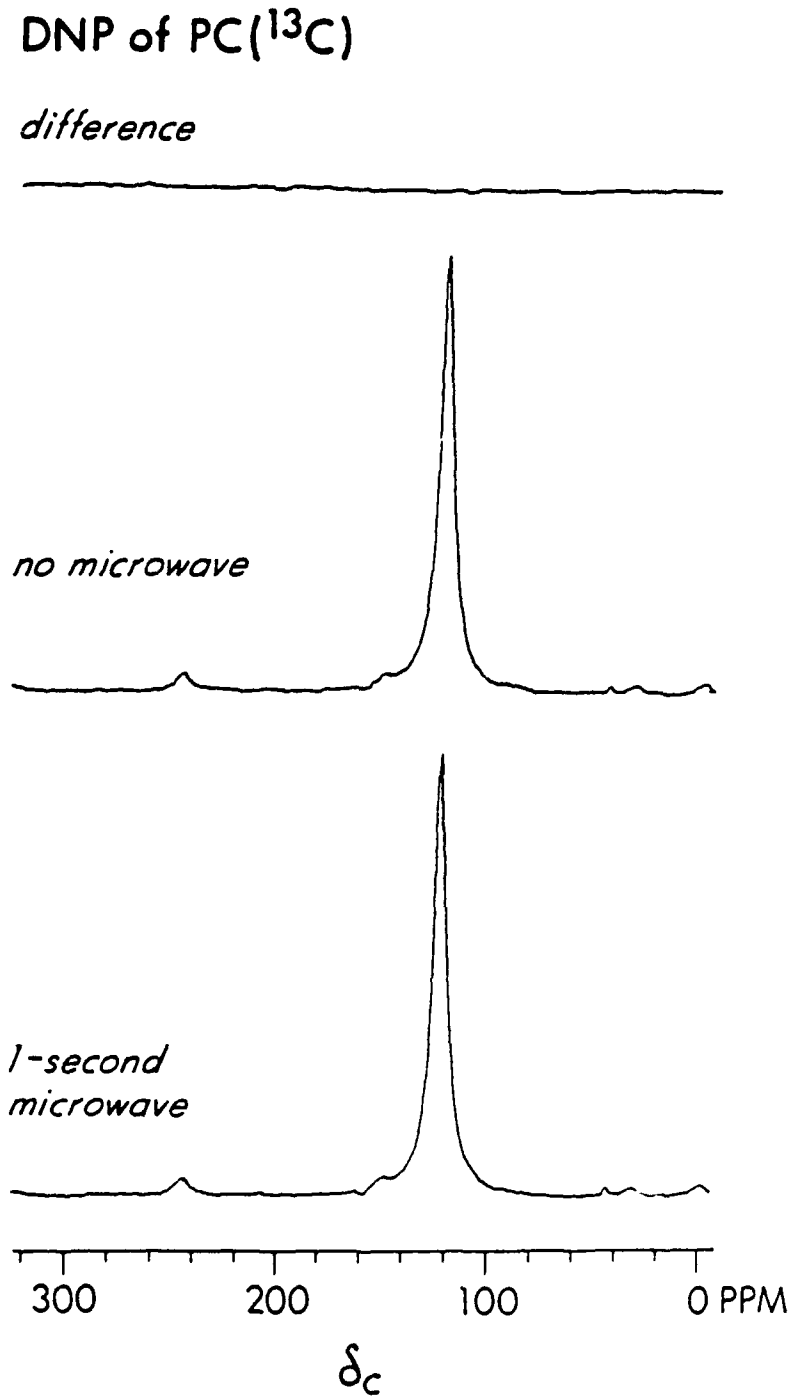
DNP of PC(^{13}C)
difference
no microwave
1-second microwave
300
200
100
0 PPM
δ_C

Figure 12

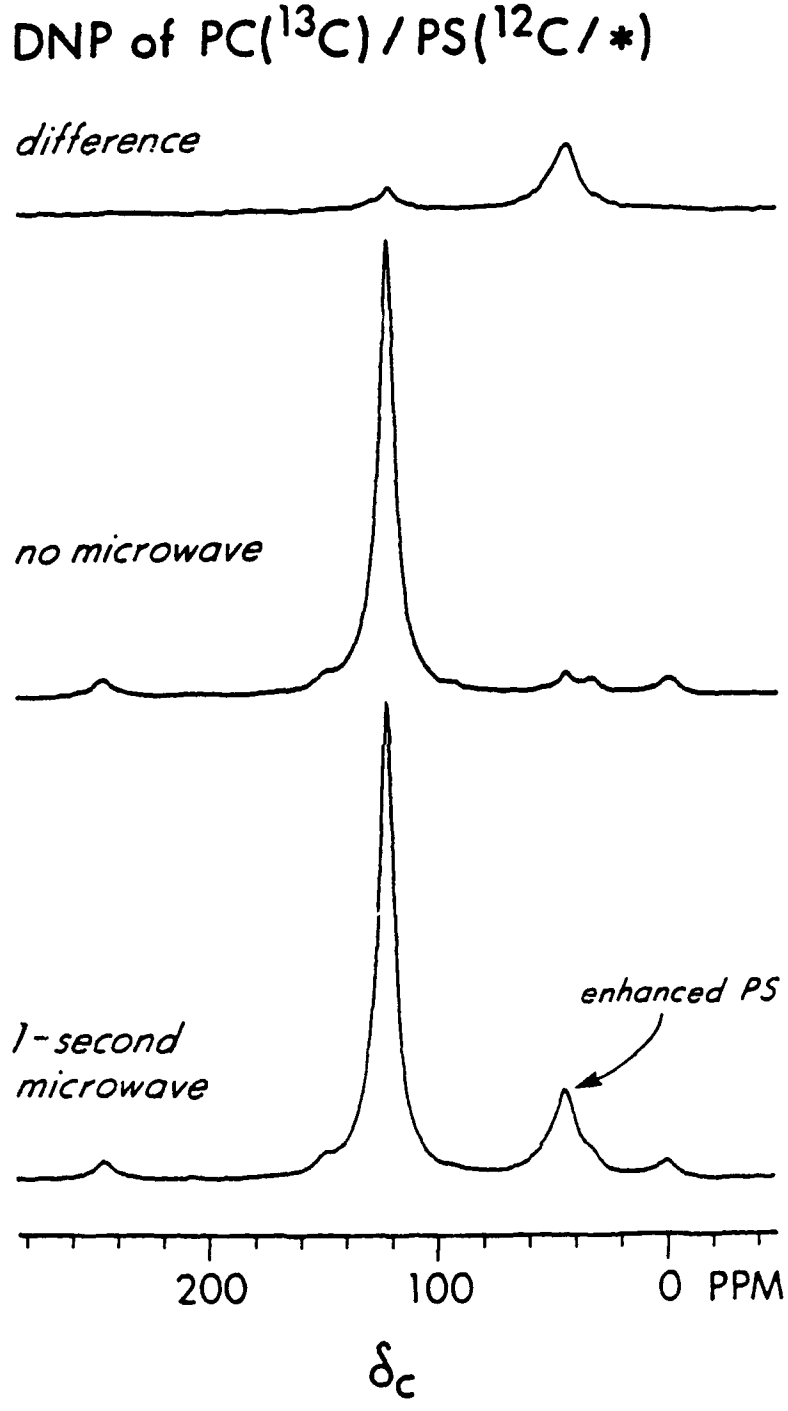
DNP of PC(^{13}C) / PS(^{12}C / *)
difference
no microwave
1-second microwave
enhanced PS
200
100
0 PPM
δ_C

Figure 13

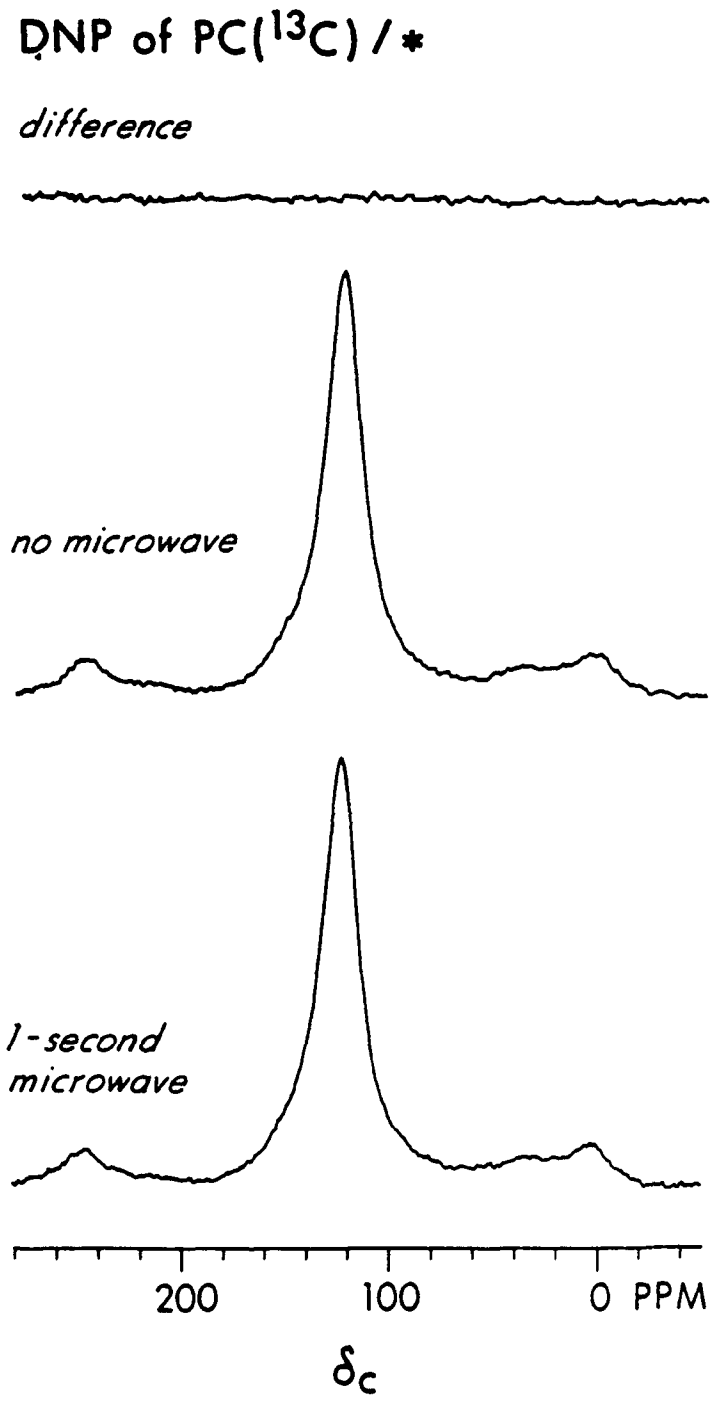
DNP of PC(13C)/*
difference
no microwave
1-second
microwave
200
100
0 PPM
δc

Figure 14

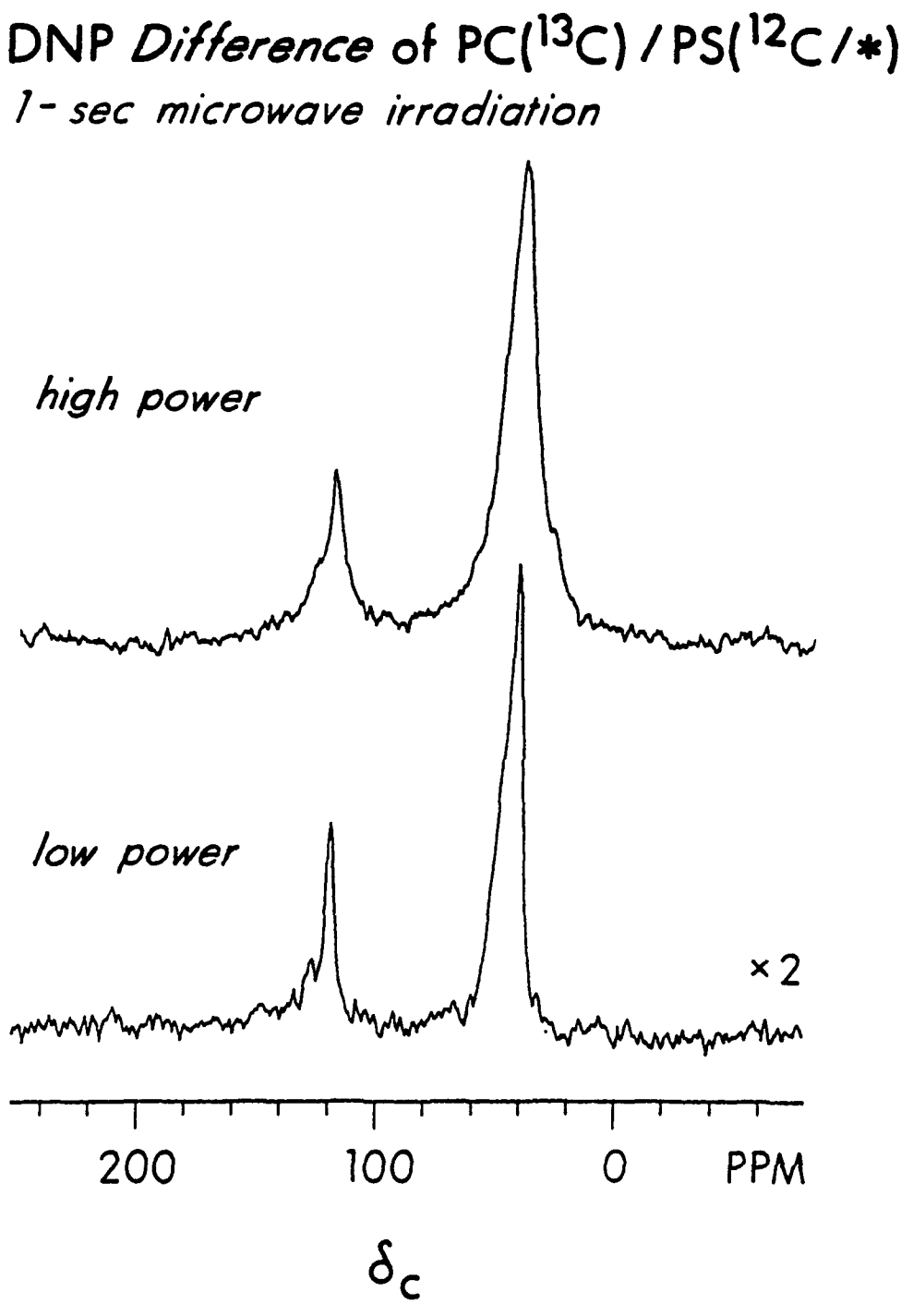
DNP Difference of PC(13C) / PS(12C/*)
1- sec microwave irradiation
high power
low power
×2
200
100
0
PPM
δc

TECHNICAL REPORT DISTRIBUTION LIST - GENERAL

Office of Naval Research (2)
Chemistry Division, Code 1113
800 North Quincy Street
Arlington, Virginia 22217-5000

Commanding Officer (1)
Naval Weapons Support Center
Dr. Bernard E. Douda
Crane, Indiana 47522-5050

Dr. Richard W. Drisko (1)
Naval Civil Engineering Laboratory
Code L52
Port Hueneme, CA 93043

David Taylor Research Center (1)
Dr. Eugene C. Fischer
Annapolis, MD 21402-5067

Dr. James S. Murday (1)
Chemistry Division, Code 6100
Naval Research Laboratory
Washington, D.C. 20375-5000

Dr. Robert Green, Director (1)
Chemistry Division, Code 385
Naval Weapons Center
China Lake, CA 93555-6001

Chief of Naval Research (1)
Special Assistant for Marine Corps Matters
Code 00MC
800 North Quincy Street
Arlington, VA 22217-5000

Dr. Bernadette Eichinger (1)
Naval Ship Systems Engineering Station
Code 053
Philadelphia Naval Base
Philadelphia, PA 19112

Dr. Sachio Yamamoto (1)
Naval Ocean Systems Center
Code 52
San Diego, CA 92152-5000

Dr. Harold H. Singerman (1)
David Taylor Research Center
Code 283
Annapolis, MD 21402-5067

In preparing the general distribution list for the TECHNICAL REPORTS, the address for the Defense Technical Information Center (DTIC) was omitted. When technical reports are prepared, two high quality copies should be forwarded to:

Defense Technical Information Center
Building 5, Cameron Station (2)
Alexandria, VA 22314